

# Study of parallel operation single phase H-bridge CSI and H-bridge VSI

Suroso, Winasis, Retno Supriyanti

Department of Electrical Engineering, Jenderal Soedirman University, Central of Java, Indonesia

## Article Info

### Article history:

Received Aug 12, 2024

Revised Dec 30, 2024

Accepted Mar 1, 2025

### Keywords:

Energy conversion

Parallel operation

Power inverter

Single-phase

Total harmonic distortion

## ABSTRACT

In some applications, parallel operation of some single-phase inverters with different characteristics is a necessity, such as in a photovoltaic power conversion system. Each power inverter with its power source works, delivering power to a common load which cannot be supplied by a single power inverter. This paper proposed a novel parallel operation of two different power inverter circuit types. H-bridge voltage source inverter (HB-VSI) and H-bridge current source inverter (HB-CSI), supplying AC power to a common load. The proposed inverter system was examined and its operation characteristics were analyzed using computer simulation. Moreover, a laboratory prototype of the inverter system was made and examined to validate some principal characteristics of the inverter system experimentally. Test results showed that by combining the HB-VSI and HB-CSI, a lower distortion of load current was achieved, specifically, total harmonic distortion (THD) of  $I_{load}$  was less than 1%. This phenomenon happens even the THD of AC currents generated by HB-VSI and HB-CSI at 6.95% and 6.18%, respectively.

This is an open access article under the [CC BY-SA](#) license.



## Corresponding Author:

Suroso

Department of Electrical Engineering, Jenderal Soedirman University

Mayjen Sungkono St. Km. 5, Blater, Purbalingga, Central of Java 53371, Indonesia

Email: suroso.te@unsoed.ac.id

## 1. INTRODUCTION

Nowadays, power inverters play a crucial role in processing the power generated by renewable energy sources. They are enabling the incorporation of renewable energy with existing electrical power grids, and even in standalone power systems, making them a fundamental component of modern energy infrastructure [1]-[4]. They convert DC power, typically from a solar panel array, battery storage system, or other DC sources, into AC power suitable for use in homes, businesses, or grid-connected applications [5], [6]. Based on the phase number, the power inverter circuits are categorized into two main types, i.e., three-phase and single-phase inverters. The three-phase inverter usually handles high power applications with three-phase AC circuits, while single-phase power inverters are applied in lower power applications [7]. Single-phase power inverters are usually implemented in residential PV systems, where a single-phase AC system is standard for household appliances and lighting. They come in various sizes (rated in several kilowatts, kW) to match the output power of the solar array as a DC source [8]-[10].

The H-bridge voltage source inverter (HB-VSI) topology is composed of four switches connected in an "H" configuration. These switches can be thyristors, IGBTs, or MOSFETs. The switches are connected to form two pairs: upper and lower switches [11]-[13]. The HB-VSI requires a DC power source, which could be a battery bank, a DC bus from a renewable energy source like solar panels or wind turbines, or a rectified AC supply. The switches in the upper and lower arms of the HB-VSI are controlled in a manner that allows

for switching of polarity across the load (typically an inductive load such as a motor or a transformer's primary winding). By controlling the switching sequence and timings of these switches, the HB-VSI can synthesize a sinusoidal AC output waveform. The AC output voltage waveform is typically controlled by implementing a pulse width modulation (PWM) waveform. By adjusting the duty cycle of PWM signals applied to the H-bridge switches, the effective value of AC output voltage can be varied, thus controlling the magnitude of the AC output [14], [15].

An H-bridge current source inverter (HB-CSI) is another type of power converter used for altering DC power to be AC power, but it operates on a different principle compared to the HB-VSI. Similar to the HB-VSI, the HB-CSI also uses four switches arranged in an "H" configuration. However, the power switches in the HB-CSI are unidirectional current switches. These switches are typically unidirectional current IGBTs or power MOSFETs, achieved by connecting discrete diodes in series. Unlike an HB-VSI, which requires a constant voltage DC source, the HB-CSI requires a constant current DC source. This DC current is often provided by DC current generation circuits [16]-[19]. Alike to the HB-VSI, PWM techniques are applied to regulate the output waveform. However, in an HB-CSI, the PWM control adjusts the width of pulses to control the average current flowing through the load rather than controlling the voltage directly. HB-CSI inherently provides protection of short-circuit faults due to its power inductor in the circuits. If a short circuit occurs, the inductor of the inverter automatically limits the current flow, protecting the circuit. In some renewable energy applications, HB-CSI can be used as a grid-tied inverter, especially in scenarios where current source characteristics are advantageous [20], [21].

In practical applications, parallel operation of some single-phase inverters offers advantages such as allowing for easy scalability of power output by adding more inverters and providing redundancy in critical applications. Operating power inverters in parallel refers to connecting multiple inverters together to achieve higher power output or a redundancy function to increase reliability [22], [23]. Each inverter typically has its own DC input from separate DC sources (such as batteries or solar arrays). Inverters in parallel should share the load proportionally based on their rated capacities. Load sharing can be achieved through control algorithms that adjust the output of each inverter based on the measured load and the available capacity of each inverter [24]-[27]. Grid-tied solar PV systems often use multiple inverters in parallel to handle larger arrays or to comply with grid connection standards [28]-[31].

Currently, the voltage source inverters (VSIs) types are widely available commercially. However, with some features and advantages which cannot be found in the VSI type, the current source inverters (CSIs) are a very potential inverter candidate for power converters of renewable energy sources, particularly in PV system applications [32]-[34]. Figure 1 presents a configuration of three single-phase inverters for a PV conversion system. The arrow sign represents the power flow direction. Different types of inverters with different characteristics are very possible to be applied in this system. Operation in parallel of single-phase inverters is commonly conducted for the same inverter type, i.e., between VSIs or between CSIs. Based on the author's literature investigation, there is no reference that discusses the operation of different inverter types, especially between the HB-VSI and HB-CSI operated in parallel. A characteristic study of this new inverter system is required in order to support the operation design of the inverter system considerably needed, such as in a renewable energy conversion system. In this paper, a novel parallel operation between two distinct inverter types, i.e., H-bridge VSI and H-bridge CSI, was proposed and investigated to explore its characteristic operation. The developed parallel inverter system was tested and examined through computer simulation and experimentally in a laboratory using a laboratory prototype.

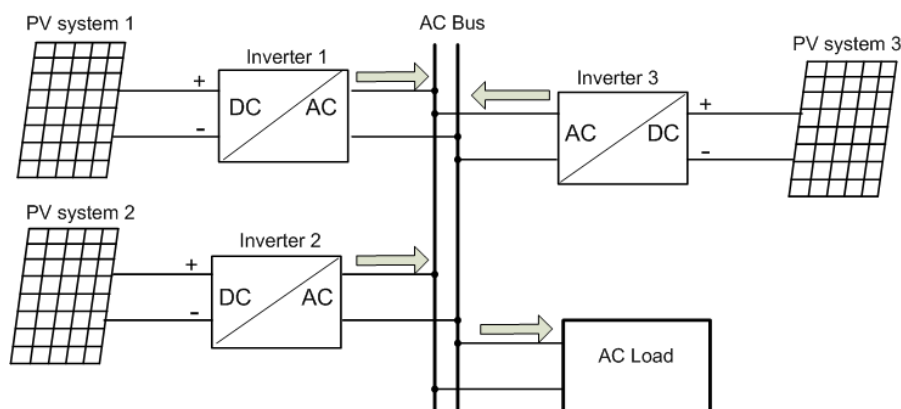


Figure 1. System diagram of parallel inverters for photovoltaic conversion

## 2. PROPOSED INVERTER SYSTEM

Circuit configuration of the H-bridge CSI is presented in Figure 2. It consists of four IGBTs and diodes to form a unidirectional current of active power switches. Controlling the switching states of these four switches, i.e.,  $Q_1Q_2Q_3Q_4$ , will generate a three-level AC current waveform as depicted in Table 1. On the other hand, the circuit of the H-bridge VSI is presented in Figure 3. By operating the switching states as shown in Table 2, a three-level AC voltage waveform is produced. Even the active switch number is the same. However, the principal operation of both circuits is different. The current source inverter proceeds the DC current as input of the circuits, while the HB-VSI processes the DC voltage source into AC power. During the switching operation, a short circuit is prohibited in the HB-VSI, while an open circuit is prohibited in the HB-CSI.

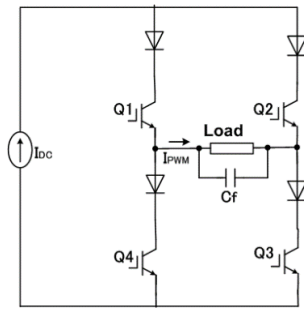


Figure 2. Circuit of H-bridge CSI [16]

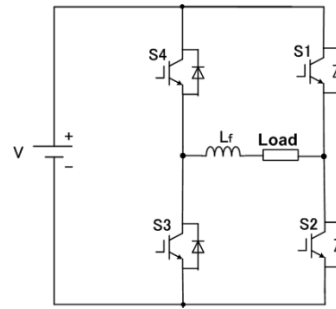


Figure 3. Circuit of H-bridge VSI [15]

Table 1. Switching states of HB-CSI

$Q_1$	$Q_2$	$Q_3$	$Q_4$	$I_{out}$
1	0	1	0	+I
1	0	0	1	0
0	1	1	0	0
0	1	0	1	-I

Table 2. Operation mode of H-bridge VSI

$S_1$	$S_2$	$S_3$	$S_4$	$I_{out}$
0	1	0	1	+V
1	0	0	1	0
0	1	1	0	0
1	0	1	0	-V

Figure 4 presents the developed parallel circuits of HB-VSI and HB-CSI. An HB-CSI consists of four unidirectional controlled switches  $Q_1Q_2Q_3Q_4$  connected with a DC current source as input power and a capacitor  $C_f$  as a filter. The H-bridge VSI composed by power switches  $S_1S_2S_3S_4$  with a DC voltage source  $V$  as input power and filter  $L_f$  at output terminal. Both inverters work together, supplying power to a common AC power load as load current ( $I_{load}$ ). The current supplied by H-bridge CSI is marked as  $I_{csi}$ , while the current drawn from H-bridge VSI is indicated as  $I_{vsi}$  as shown in Figure 4. The DC current generator of HB-CSI was implemented by a power switch ( $Q_c$ ), diode  $D_c$  and an inductor  $L$  with a current sensor to facilitate controlling its current magnitude as shown in Figure 5. In order to regulate the current delivered by the H-bridge CSI, a proportional plus integral (PI) current regulator was implemented as shown in Figure 6(a). A current sensor is utilized to quantify the current in the inductor to be controlled as DC input current of the H-bridge CSI. The sinusoidal PWM was applied to produce a lower distortion AC output current of the H-bridge CSI as described in Figure 6(b).

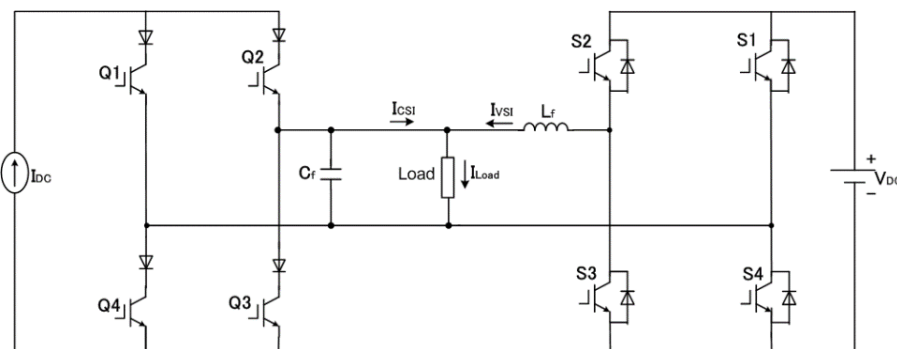


Figure 4. Proposed parallel circuits of H-bridge VSI and CSI inverters

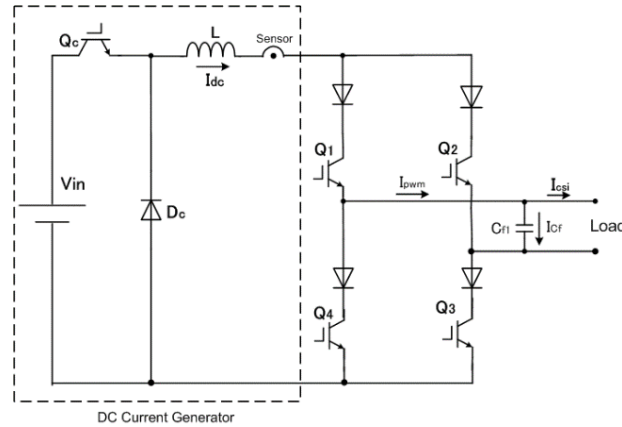


Figure 5. H-bridge CSI with DC current generator circuits [19]

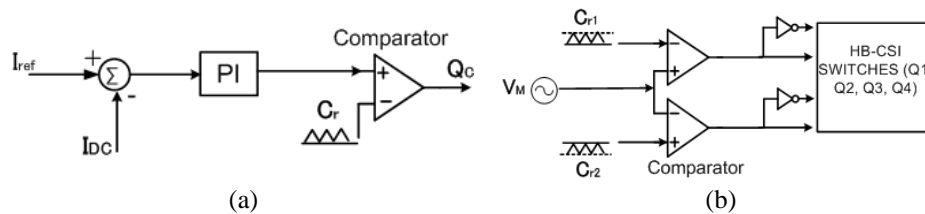


Figure 6. Control circuits: (a) current control of H-bridge CSI and (b) PWM modulation control circuit [29]

Moreover, the current controller of HB-VSI is depicted in Figure 7. By using a current sensor at its output terminal, the AC output current of the H-bridge VSI was measured as  $I_{vsi}$ . This signal was compared with the reference AC current  $I_{ref}$  of the H-bridge VSI. The PI current controller with a limiter and two triangular carrier signals was applied to process the error signals to generate PWM gating signals of the four H-bridge VSI power switches. The AC output current of the HB-CSI and HB-VSI was synchronized by using their sinusoidal modulating signal ( $V_M$ ) of the PWM strategy.

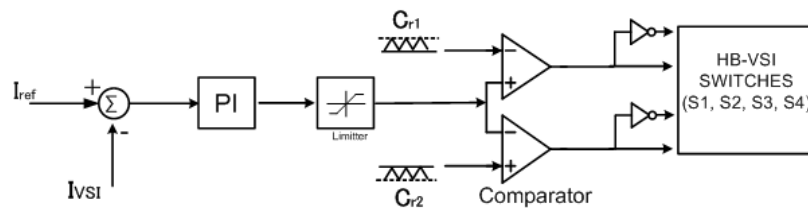


Figure 7. Current control of H-bridge VSI

### 3. TEST RESULTS AND DISCUSSION

#### 3.1. Computer simulation test

The basic principle of operation of the developed inverter system was examined by using the computer software of PSIM. Table 3 presents circuit parameters of the HB-CSI. The inductance of the inductor to generate DC current was 1 mH. The operation frequency of the inverter switches was 22 kHz with 50 Hz as the main AC current frequency. The H-bridge CSI was connected to a filter capacitor 14  $\mu$ F before being connected to a power load resistor 3.3  $\Omega$  in series with an inductor 1 mH. Moreover, the circuit parameters of HB-VSI are listed in Table 4. The DC input voltage source was 24 V. The working frequency of switches and the main output frequency were the same of the HB-CSI, i.e., 22 kHz and 50 Hz, respectively. The output inductor filter was 1 mH. The H-bridge VSI was connected to a common power load together with the H-bridge CSI, i.e.,  $R = 3.3 \Omega$ ,  $L = 1 \text{ mH}$ .

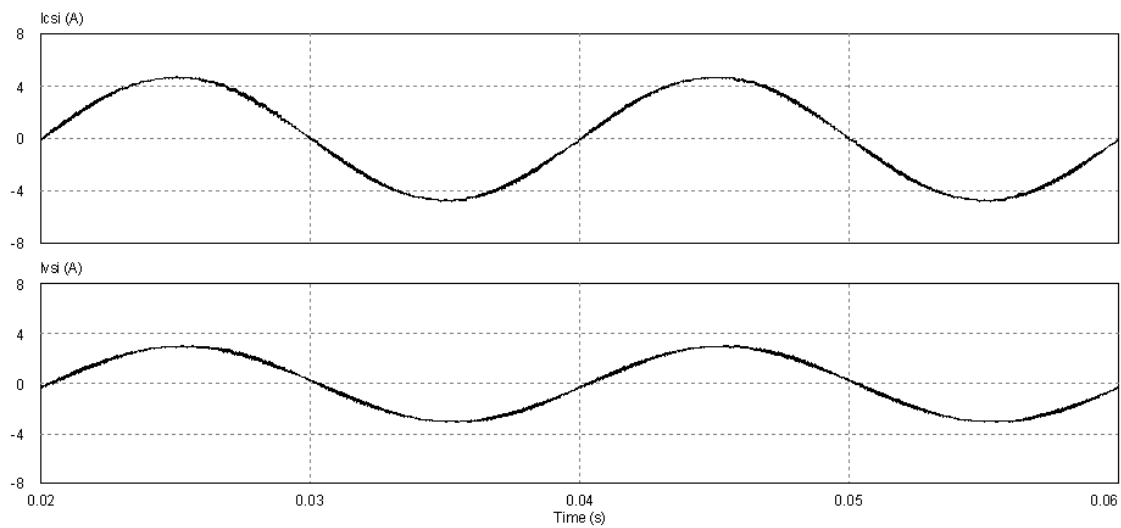
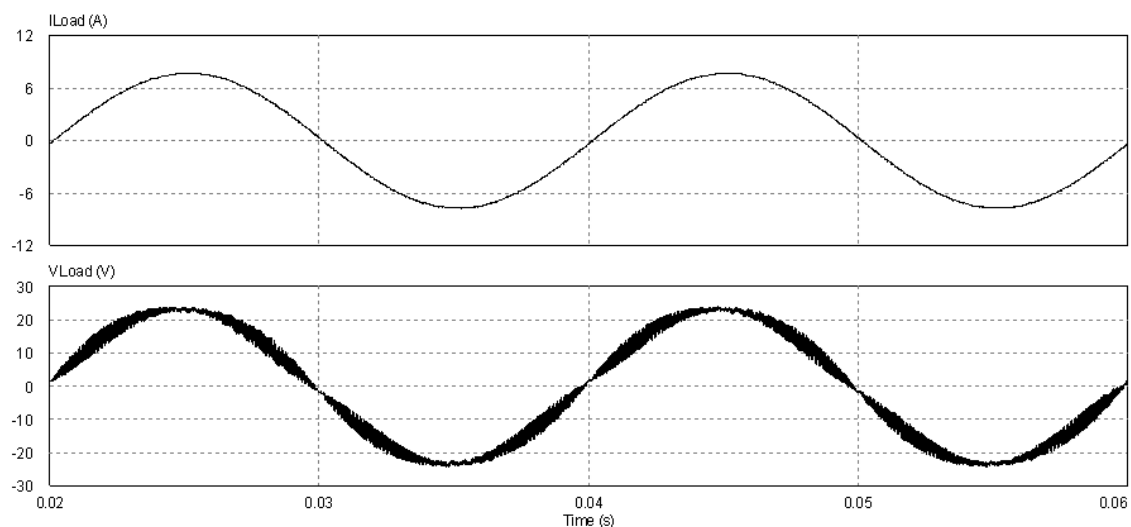
Table 3. Circuit parameters of HB-CSI

Parameters	Values
Inductance of DC inductor L	1 mH
Capacitor filter	14 $\mu$ F
Switching frequency of IGBT	22 kHz
Main frequency	50 Hz
Connected power load	R = 3.3 $\Omega$ , L = 1 mH

Table 4. Circuit parameters of HB-VSI

Parameters	Values
Power reactor of the filter	1 mH
DC voltage source	24 V
Switching frequency of the IGBT	22 kHz
Main frequency	50 Hz
Connected power load	R = 3.3 $\Omega$ , L = 1 mH

Figure 8 shows the current waveform of HB-CSI ( $I_{csi}$ ) and H-bridge VSI ( $I_{vsi}$ ) at different magnitudes. Both inverters produced sinusoidal output current with low waveform distortion. The load current ( $I_{load}$ ) and load voltage waveform ( $V_{load}$ ) are presented in Figure 9. A sinusoidal load current waveform was produced in this test. In order to analyze harmonic components and distortions of current waveforms in more detail, an analysis of the fast Fourier transform (FFT) was conducted by using a computer simulation. Figure 10 shows the low-frequency harmonics of AC current generated by the H-bridge CSI. The magnitudes of all harmonic components were less than 5%. It can be observed in this figure that the magnitudes of the 3<sup>rd</sup>, 5<sup>th</sup>, and 7<sup>th</sup> were 0.3%, 0.1% and 0.08% respectively.

Figure 8. Current form H-bridge CSI ( $I_{csi}$ ) and H-bridge VSI ( $I_{vsi}$ )Figure 9. Load current ( $I_{load}$ ) and load voltage ( $V_{load}$ ) waveforms

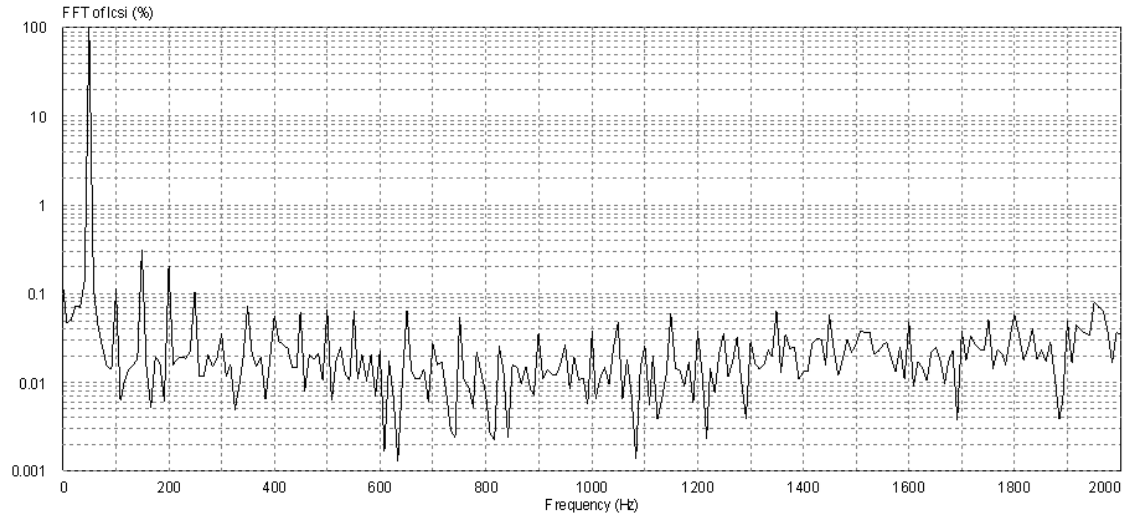


Figure 10. Harmonics spectra of H-bridge CSI output current ( $I_{CSI}$ )

Moreover, using the same method of FFT analysis, the low-frequency harmonics profile of AC output current produced by the H-bridge VSI is depicted in Figure 11. In these results, all harmonic components were less than 0.4%. The magnitudes of the 3<sup>rd</sup>, 5<sup>th</sup>, and 7<sup>th</sup> harmonic orders were 0.08%, 0.1% and 0.99%, respectively. Harmonic spectra of the load current supplied by both inverters are presented in Figure 12. As can be viewed in this figure, the magnitudes of all harmonic components were less than 0.3%. The 3<sup>rd</sup>, 5<sup>th</sup>, and 7<sup>th</sup> harmonic orders were 0.2%, 0.1% and 0.07% respectively. The harmonic characteristics of load current were much better than the harmonic contents of AC currents generated by the HB-CSI and HB-VSI, as shown in Figure 13. Although the THD values of HB-VSI and HB-CSI were more than 1%, the THD percentage of the load current was always less than 1%. It is a great feature for AC power loads requiring high power quality of AC current supplied by power inverters.

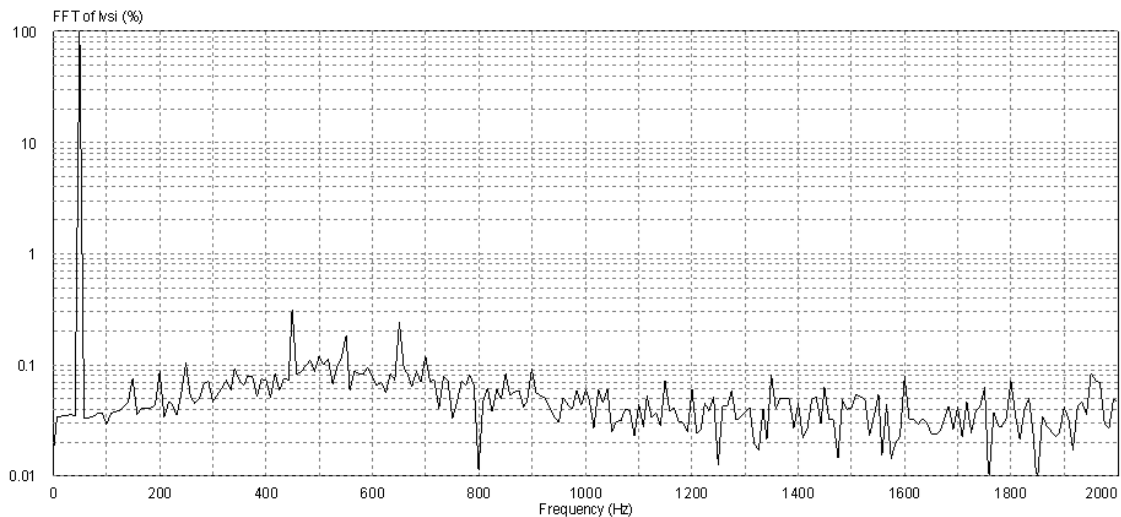


Figure 11. Harmonic spectra of H-bridge VSI output current ( $I_{VSI}$ )

### 3.2. Experiment test results

To verify the inverter system experimentally, laboratory prototypes of the HB-CSI and H-bridge VSI were made and tested. The power switches of the HB-CSI circuits were realized using IGBTs of FGA25N120ANTD connected in series with an ultrafast diode STTH6012. The IGBTs of

FGA25N120ANTD were also implemented to construct the H-bridge VSI. The circuit parameters were the same in the computer simulation test of Tables 3 and 4. Figure 14 presents the measured waveforms of load current ( $I_{load}$ ) and the current supplied by H-bridge CSI ( $I_{csi}$ ) during the operation in parallel of H-bridge CSI and H-bridge VSI. The current injected by the H-bridge VSI is shown in Figure 15. Both inverters supplied a sinusoidal current to the load experimentally. The waveform of the load voltage is depicted in Figure 16. Low distortion of the load current waveform was confirmed experimentally.

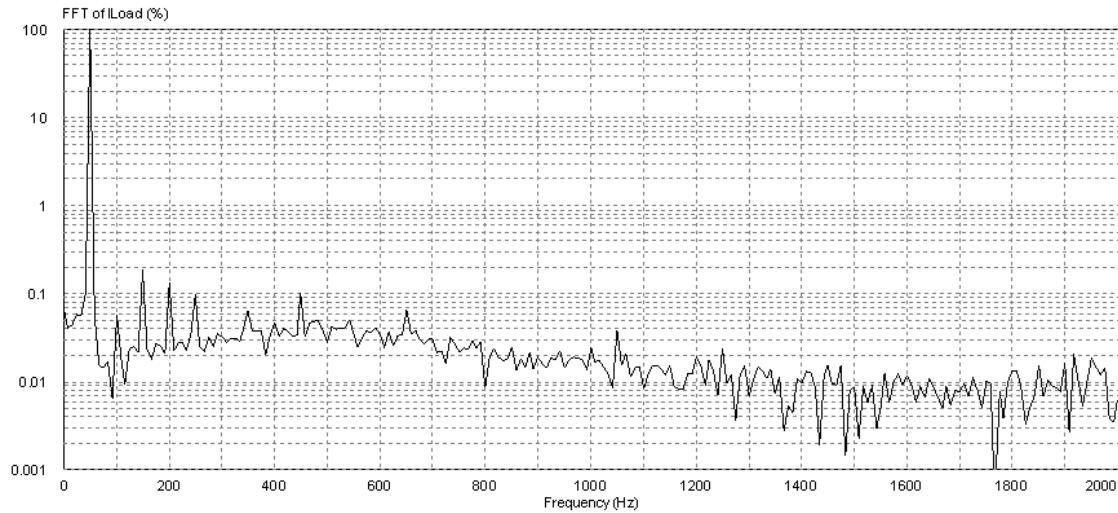


Figure 12. Harmonics profile of load current ( $I_{load}$ )

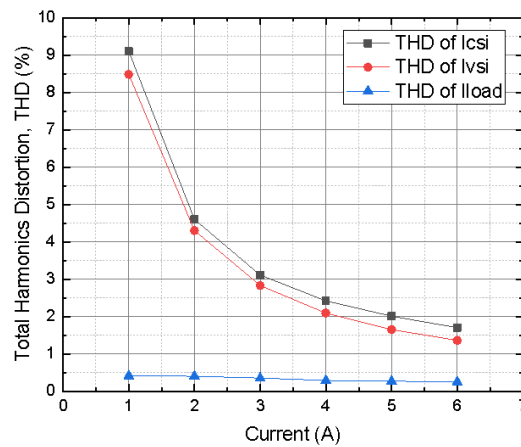


Figure 13. Harmonics profile comparison of  $I_{csi}$ ,  $I_{vsi}$ , and  $I_{load}$

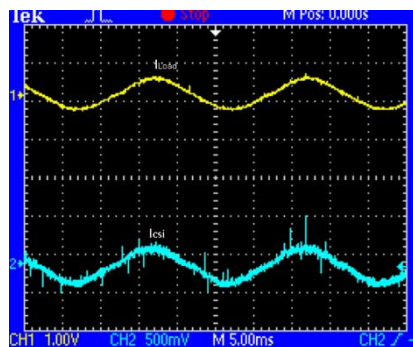


Figure 14. Load current ( $I_{load}$ ) and H-bridge CSI output current ( $I_{csi}$ )

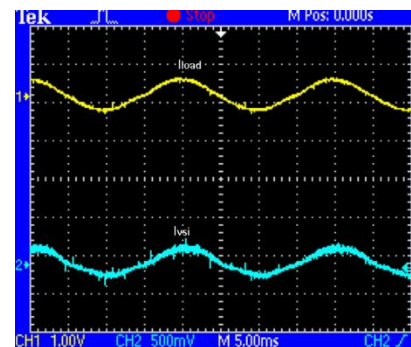


Figure 15. Load current ( $I_{load}$ ) and H-bridge VSI output current ( $I_{vsi}$ )



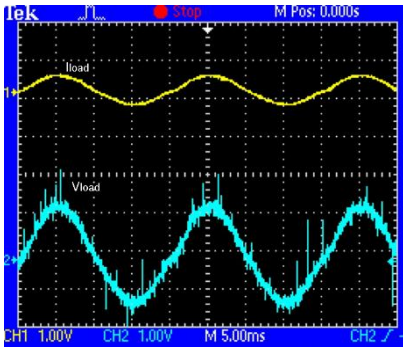


Figure 16. Load current ( $I_{load}$ ) and load voltage ( $V_{load}$ ) waveforms

4. CONCLUSION

In this research paper, a new parallel operation of H-bridge CSI and H-bridge VSI was presented and discussed to investigate its basic operation characteristics. By using computer testing software and laboratory prototype test results, it was verified that the proposed inverter system worked well, generating sinusoidal load currents from both different inverters. The test results revealed a new feature that the total harmonics distortion (THD) of the AC current flowing through the common power load was much lower than the THD value of the AC current supplied by either H-bridge CSI or H-bridge VSI. This condition is a new advantage obtained from the parallel operation of the H-bridge CSI and H-bridge VSI.

ACKNOWLEDGEMENTS

The authors would like to express their sincere appreciation to LPPM Jenderal Soedirman University, and the Directorate General of Higher Education, Ministry of Education, Culture, Research and Technology, Indonesia, for their financial support of this research project. Their funding played a crucial role in the successful execution of this study and the attainment of our research goals. Furthermore, the authors are grateful to my research team members and collaborators who have contributed their time, expertise, and efforts to this project.

FUNDING INFORMATION

This work was funded by a research grant provided by the Regular Fundamental Research Scheme, Directorate General of Higher Education, Ministry of Education, Culture, Research and Technology, Indonesia in 2024 with contract number 20.4/UN23.35.5/PT.01.00/VI/2024.

AUTHOR CONTRIBUTIONS STATEMENT

This journal uses the Contributor Roles Taxonomy (CRediT) to recognize individual author contributions, reduce authorship disputes, and facilitate collaboration.

Name of Author	C	M	So	Va	Fo	I	R	D	O	E	Vi	Su	P	Fu
Suroso	✓	✓	✓	✓	✓	✓	✓	✓	✓	✓	✓	✓	✓	✓
Winasis				✓	✓		✓			✓				
Retno Supriyanti					✓		✓			✓				

C : Conceptualization	I : Investigation	Vi : Visualization
M : Methodology	R : Resources	Su : Supervision
So : Software	D : Data Curation	P : Project administration
Va : Validation	O : Writing - Original Draft	Fu : Funding acquisition
Fo : Formal analysis	E : Writing - Review & Editing	

CONFLICT OF INTEREST STATEMENT

Authors state no conflict of interest.



## DATA AVAILABILITY

The data that support the findings of this study are available from the corresponding author, [S], upon reasonable request.





## REFERENCES

- [1] C. Breyer *et al.*, "On the history and future of 100% renewable energy systems research," *IEEE Access*, vol. 10, pp. 78176–78218, 2022, doi: 10.1109/ACCESS.2022.3193402.
- [2] J. Jurasz, F. A. Canales, A. Kies, M. Guezgouz, and A. Beluco, "A review on the complementarity of renewable energy sources: Concept, metrics, application and future research directions," *Solar Energy*, vol. 195, pp. 703–724, Jan. 2020, doi: 10.1016/j.solener.2019.11.087.
- [3] S. Wang, "Current status of PV in China and its future forecast," *CSEE Journal of Power and Energy Systems*, vol. 6, no. 1, pp. 72–82, Mar. 2020, doi: 10.17775/CSEEJPES.2019.03170.
- [4] A. Gholami, M. Ameri, M. Zandi, R. G. Ghoachani, S. Eslami, and S. Pierfederici, "Photovoltaic potential assessment and dust impacts on photovoltaic systems in Iran: Review paper," *IEEE Journal of Photovoltaics*, vol. 10, no. 3, pp. 824–837, May 2020, doi: 10.1109/JPHOTOV.2020.2978851.
- [5] J. Wang, K. Sun, H. Wu, L. Zhang, J. Zhu, and Y. Xing, "Quasi-two-stage multifunctional photovoltaic inverter with power quality control and enhanced conversion efficiency," *IEEE Transactions on Power Electronics*, vol. 35, no. 7, pp. 7073–7085, Jul. 2020, doi: 10.1109/TPEL.2019.2956940.
- [6] Z. Xiang *et al.*, "A residential miniboot photovoltaic inverter with maximum power point operation and power quality compensation," *IEEE Transactions on Industrial Electronics*, vol. 70, no. 5, pp. 4320–4331, May 2023, doi: 10.1109/TIE.2022.3187573.
- [7] J. Wang, H. Wu, T. Yang, L. Zhang, and Y. Xing, "Bidirectional three-phase DC–AC converter with embedded DC–DC converter and carrier-based PWM strategy for wide voltage range applications," *IEEE Transactions on Industrial Electronics*, vol. 66, no. 6, pp. 4144–4155, Jun. 2019, doi: 10.1109/TIE.2018.2866080.
- [8] S. B. Kjaer, J. K. Pedersen, and F. Blaabjerg, "A review of single-phase grid-connected inverters for photovoltaic modules," *IEEE Transactions on Industry Applications*, vol. 41, no. 5, pp. 1292–1306, Sep. 2005, doi: 10.1109/TIA.2005.853371.
- [9] K. Alluhaybi, I. Batarseh, and H. Hu, "Comprehensive review and comparison of single-phase grid-tied photovoltaic microinverters," *IEEE Journal of Emerging and Selected Topics in Power Electronics*, vol. 8, no. 2, pp. 1310–1329, 2020, doi: 10.1109/JESTPE.2019.2900413.
- [10] J. M. Carrasco *et al.*, "Power-electronic systems for the grid integration of renewable energy sources: A survey," *IEEE Transactions on Industrial Electronics*, vol. 53, no. 4, pp. 1002–1016, Jun. 2006, doi: 10.1109/TIE.2006.878356.
- [11] P. K. Behera, A. Satpathy, and M. Pattnaik, "Design and implementation of a single-band hysteresis current controlled H-bridge inverter," in *2020 3rd International Conference on Energy, Power and Environment: Towards Clean Energy Technologies*, IEEE, Mar. 2021, pp. 1–6, doi: 10.1109/ICEPE50861.2021.9404454.
- [12] M. Munir, Wisyahyadi, A. Rizqian, and J. Furqani, "Inherently sinusoidal single-phase voltage source inverter based on modified cuk cell," *Chinese Journal of Electrical Engineering*, vol. 10, no. 1, pp. 114–123, Mar. 2024, doi: 10.23919/CJEE.2024.000051.
- [13] R. Panigrahi, S. K. Mishra, S. C. Srivastava, A. K. Srivastava, and N. N. Schulz, "Grid integration of small-scale photovoltaic systems in secondary distribution network—A review," *IEEE Transactions on Industry Applications*, vol. 56, no. 3, pp. 3178–3195, May 2020, doi: 10.1109/TIA.2020.2979789.
- [14] M. Kumar, "Open circuit fault detection and switch identification for LS-PWM H-bridge inverter," *IEEE Transactions on Circuits and Systems II: Express Briefs*, vol. 68, no. 4, pp. 1363–1367, Apr. 2021, doi: 10.1109/TCSII.2020.3035241.
- [15] A. Bandyopadhyay, K. Mandal, and S. Parui, "Design-oriented dynamical analysis of single-phase H-bridge inverter," in *2020 IEEE International Conference on Power Electronics, Smart Grid and Renewable Energy (PESGRE2020)*, IEEE, Jan. 2020, pp. 1–6, doi: 10.1109/PESGRE45664.2020.9070760.
- [16] Suroso and T. Noguchi, "Multilevel current waveform generation using inductor cells and H-bridge current-source inverter," *IEEE Transactions on Power Electronics*, vol. 27, no. 3, pp. 1090–1098, 2012, doi: 10.1109/TPEL.2010.2056933.
- [17] Z. Bai and Z. Zhang, "Conformation of multilevel current source converter topologies using the duality principle," *IEEE Transactions on Power Electronics*, vol. 23, no. 5, pp. 2260–2267, Sep. 2008, doi: 10.1109/TPEL.2008.2001893.
- [18] K. Kim, H. Cha, and H.-G. Kim, "A new single-phase switched-coupled-inductor DC–AC inverter for photovoltaic systems," *IEEE Transactions on Power Electronics*, vol. 32, no. 7, pp. 5016–5022, Jul. 2017, doi: 10.1109/TPEL.2016.2606489.
- [19] Suroso, Winasis, and T. Noguchi, "Overlap-time compensation technique for current-source power inverter," *IET Power Electronics*, vol. 13, no. 4, pp. 854–862, Mar. 2020, doi: 10.1049/iet-pel.2019.0503.
- [20] F. Luo, G. Ranzi, C. Wan, Z. Xu, and Z. Y. Dong, "A multistage home energy management system with residential photovoltaic penetration," *IEEE Transactions on Industrial Informatics*, vol. 15, no. 1, pp. 116–126, Jan. 2019, doi: 10.1109/TII.2018.2871159.
- [21] L. Callegaro, G. Konstantinou, C. A. Rojas, N. F. Avila, and J. E. Fletcher, "Testing evidence and analysis of rooftop PV inverters response to grid disturbances," *IEEE Journal of Photovoltaics*, vol. 10, no. 6, pp. 1882–1891, Nov. 2020, doi: 10.1109/JPHOTOV.2020.3014873.
- [22] A. Sinha and K. C. Jana, "Comprehensive review on control strategies of parallel-interfaced voltage source inverters for distributed power generation system," *IET Renewable Power Generation*, vol. 14, no. 13, pp. 2297–2314, Oct. 2020, doi: 10.1049/iet-rpg.2019.1067.
- [23] C. Song, R. Zhao, M. Zhu, and Z. Zeng, "Operation method for parallel inverter system with common DC link," *IET Power Electronics*, vol. 7, no. 5, pp. 1138–1147, May 2014, doi: 10.1049/iet-pel.2013.0411.
- [24] J. He and Y. W. Li, "An enhanced microgrid load demand sharing strategy," *IEEE Transactions on Power Electronics*, vol. 27, no. 9, pp. 3984–3995, Sep. 2012, doi: 10.1109/TPEL.2012.2190099.
- [25] A. Mohd, E. Ortjohann, D. Morton, and O. Omari, "Review of control techniques for inverters parallel operation," *Electric Power Systems Research*, vol. 80, no. 12, pp. 1477–1487, Dec. 2010, doi: 10.1016/j.epr.2010.06.009.
- [26] Z. Liu, J. Liu, X. Hou, Q. Dou, D. Xue, and T. Liu, "Output impedance modeling and stability prediction of three-phase paralleled inverters with master-slave sharing scheme based on terminal characteristics of individual inverters," *IEEE Transactions on Power Electronics*, pp. 1–1, 2015, doi: 10.1109/TPEL.2015.2483741.





- [27] S. D. Panjaitan, R. Kurnianto, B. W. Sanjaya, and M. C. Turner, "Control of parallel inverters for high power quality and sharing accuracy in single-phase AC microgrids," in *2018 UKACC 12th International Conference on Control (CONTROL)*, IEEE, Sep. 2018, pp. 50–55, doi: 10.1109/CONTROL.2018.8516761.
- [28] X. Zou, X. Du, and G. Wang, "Modeling and stability analysis for multiple parallel grid-connected inverters system," in *2018 IEEE Applied Power Electronics Conference and Exposition (APEC)*, IEEE, Mar. 2018, pp. 2431–2436, doi: 10.1109/APEC.2018.8341357.
- [29] Suroso and H. Siswanto, "Study of novel parallel H-bridge and common-emitter current-source inverters for photovoltaic power conversion system," *International Journal of Power Electronics and Drive Systems (IJPEDS)*, vol. 13, no. 1, p. 500, Mar. 2022, doi: 10.11591/ijpeds.v13.i1.pp500-508.
- [30] J. Yu, L. Deng, D. Song, and M. Pei, "Wide bandwidth control for multi-parallel grid-connected inverters with harmonic compensation," *Energies*, vol. 12, no. 3, p. 571, Feb. 2019, doi: 10.3390/en12030571.
- [31] B. John, A. Ghosh, and F. Zare, "Load sharing in medium voltage islanded microgrids with advanced angle droop control," *IEEE Transactions on Smart Grid*, vol. 9, no. 6, pp. 6461–6469, Nov. 2018, doi: 10.1109/TSG.2017.2713452.
- [32] F. Marignetti, R. L. Di Stefano, G. Rubino, and R. Giacomobono, "Current source inverter (CSI) power converters in photovoltaic systems: A comprehensive review of performance, control, and integration," *Energies*, vol. 16, no. 21, p. 7319, Oct. 2023, doi: 10.3390/en16217319.
- [33] P. G. Barbosa, H. A. C. Braga, M. D. C. B. Rodrigues, and E. C. Teixeira, "Boost current multilevel inverter and its application on single-phase grid-connected photovoltaic systems," *IEEE Transactions on Power Electronics*, vol. 21, no. 4, pp. 1116–1124, Jul. 2006, doi: 10.1109/TPEL.2006.876784.
- [34] A. Singh and B. Mirafzal, "An efficient grid-connected three-phase single-stage boost current source inverter," *IEEE Power and Energy Technology Systems Journal*, vol. 6, no. 3, pp. 142–151, Sep. 2019, doi: 10.1109/JPETS.2019.2929952.

## BIOGRAPHIES OF AUTHORS







**Suroso**     received the B. Eng. degree in electrical engineering from Gadjah Mada University, Indonesia, in 2001, and the M. Eng. degree in electrical and electronics engineering from Nagaoka University of Technology, Japan, in 2008. He was a research student at the electrical engineering department, Tokyo University, Japan, from 2005 to 2006. He earned a Ph.D. degree in the Energy and Environment Engineering Department, Nagaoka University of Technology, Japan, in 2011. He was a visiting researcher at the Electrical and Electronics Engineering Department, Shizuoka University, Japan, from 2009 to 2011. Currently, He is a Professor at the Department of Electrical Engineering, Jenderal Soedirman University, Purwokerto, Jawa Tengah, Indonesia. His research interest includes static power converters and their application in renewable energy conversion systems. He can be contacted at email: suroso.te@unsoed.ac.id.



**Winasis**     received a Bachelor of Engineering (B.Eng.) and a Master of Engineering from Gadjah Mada University, Indonesia. Currently, he is a lecturer in the Electrical Engineering Department, Jenderal Soedirman University. His research interests are power systems and renewable energy. He can be contacted at email: winasis@unsoed.ac.id.



**Retno Supriyanti**     is a Professor at the Electrical Engineering Department, Jenderal Soedirman University, Indonesia. She received her Ph.D. in March 2010 from Nara Institute of Science and Technology, Japan. Also, she received her M.S. degree and bachelor's degree in 2001 and 1998, respectively, from the Electrical Engineering Department, Gadjah Mada University, Indonesia. Her research interests include image processing, computer vision, pattern recognition, biomedical applications, E-health, tele-health, and telemedicine. She can be contacted at email: retno\_supriyanti@unsoed.ac.id.